Electronic Supplementary Information for

Recyclable magnetic covalent organic framework for the extraction of marine biotoxins

Vanesa Romero,[a,b] *Soraia P. S. Fernandes*,[a,c] *Laura Rodriguez-Lorenzo*,[a] *Yury V. Kolen'ko*,[a] *Begoña Espiña,**,[a] *Laura M. Salonen**,[a]

[a]International Iberian Nanotechnology Laboratory (INL), Av. Mestre José Veiga, 4715-330 Braga, Portugal

[b]Departamento de Química Analítica y Alimentaria, Área de Química Analítica, Facultad de Química, Universidad de Vigo, Campus As Lagoas-Marcosende, 36310 Vigo, Spain

[c]Department of Chemistry, QOPNA, University of Aveiro, Campus Universitário de Santiago, 3810-193 Aveiro, Portugal

*Corresponding Author: begona.espina@inl.int; laura.salonen@inl.int

Contents

1. Abbreviations

AE	Adsorption efficiency
APTES	3-(Aminopropyl)triethoxysilane
Aq.	Aqueous
BET	Brunauer–Emmett–Teller
BD-Me_2	*o*-Tolidine
COF	Covalent organic framework
DOPA	Dopamine
DSP	Diarrhetic shellfish poisoning
DTX-1	Dinophysistoxin-1
EDX	Energy dispersive X-ray spectroscopy
EFSA	European Food Safety Agency
FT-IR	Fourier-transform infrared
HAB	Harmful algal bloom
MSPE	Magnetic solid-phase extraction
NP	Nanoparticle
OA	Okadaic acid
OPA	*o*-Phthaldialdehyde
QSDFT	Quenched-solid density functional theory
RT	Room temperature
RSD	Relative standard deviation
SD	Standard deviation
SAXS	Small angle X-ray scattering
SEM	Scanning electron microscopy
TEF	Toxic equivalent factor
TEM	Transmission electron microscopy
TGA	Thermogravimetric analysis
Tp	Triformylphloroglucinol
VSM	Vibrating sample magnetometer
XRD	X-ray diffraction

2. Materials and Methods

Reagents and chemicals

Iron(III) chloride hexahydrate 99% and iron(II) chloride tetrahydrate 99% were purchased from Sigma Aldrich, ammonium hydroxide 25% extra pure from Acros Organics, and dopamine hydrochloride 98% from TCI.

o-Phthaldialdehyde 99% and 2-mercaptoethanol 99% from Sigma-Aldrich dissolved in absolute ethanol 99.8% from Riedel-de-Häen were used as reagents in the OPA assay. Butylamine 99% from Sigma-Aldrich was used as standard for the calibration curve. Boric acid 99.9% from Merck was used to prepare the 50 mM aq. borate buffer solution (pH 9).

Hexamethylenetetraamine 99.5% from Sigma-Aldrich, anhydrous phloroglucinol 99% from Acros Organics, and trifluoroacetic acid HPLC grade from Fischer Chemical were used for the synthesis of Tp. Commercial hydrochloric acid 37% from Fischer Chemical was used to prepare the aq. 3 M HCl solution. *o*-Tolidine 98% from TCI and dioxane extra dry 99.5% from Acros Organics were used for TpBD-Me_2 synthesis. The aq. 6 M acetic acid used as catalyst was prepared by dilution of commercial acetic acid 99.8% from EMD-Millipore.

Dichloromethane HPLC grade, tetrahydrofuran HPLC grade from Fischer Chemical (Leics, UK), and acetone 99.5% from Riedel-de-Häen (Seelze, Germany) were used for the washing of the obtained products.

Okadaic acid from *Prorocentrum* sp. was purchased from Merck-Calbiochem. 6,8-Difluoro-4-methylumbelliferyl phosphate (DiFMUP) was purchased from Molecular Probes. Protein phosphatase-1 (PP1) catalytic sub-unit (α-isoform from rabbit), synthetic ASTM seawater, and all other reagents for OA quantification were purchased from Sigma-Aldrich.

Synthesis of mTpBD-Me_2

Ultrapure water was produced by Milli-Q Advantage A10 system (Millipore; resistivity = 18.2 MΩ cm^{-1}). Pressure tubes of 100 mL (ACE glass, bushing type back seal, 17.8 cm x 38.1 mm)

and 15 mL (ACE glass, bushing type back seal,10.2 cm x 25.4 mm) were used for the pre-functionalization of Fe_3O_4@DOPA and mTpBD-Me_2 synthesis, respectively. A NdFeB magnet was used for the isolation of the magnetic nanoparticles and mTpBD-Me_2.

Characterization

Horiba Scientific Fluoromax-4 spectrofluorometer was used for fluorescent quantification of primary amine groups by OPA assay. Excitation wavelength of 336 nm was used and the emission was measured in the range 350–600 nm. Clear-sided 1 mL quartz cuvette was used for the measurements.

Infrared (IR) spectra were recorded on a Bruker VERTEX 80v FT-IR spectrometer in ATR (attenuated total reflection) mode. IR data is background-corrected and reported in frequency of absorption (cm^{-1}).

Small and wide angle X-ray scattering (SAXS) measurements were performed on an Anton Paar SAXSess mc2 instrument operating at 40 kV and 50 mA. Data were collected with an image plate detector. Samples were placed in a holder with Mylar windows for the measurement. Data are background corrected.

X-Ray diffraction (XRD) analyses were performed on a PANanlytical X'Pert PRO MRD diffractometer operating at 45 kV and 40 mA.

Thermogravimetric analyses (TGA) were carried out using a TGA/DSC 1 STAR^e system from Mettler Toledo. The sample was heated from 30 °C to 900 °C with a heating rate of 5 °C min^{-1} under Ar atmosphere.

Nitrogen sorption measurements were carried out at 77 K using a Quantachrome Autosorb IQ2 automated analyzer. Powder samples were outgassed by heating to 120 °C (heating rate: 5 °C min^{-1}, dwell time: 720 min). Surface areas were estimated by the multipoint Brunauer–Emmett–Teller (BET) method using ASiQwin(TM) software. Pore size distributions

were estimated using quenched-solid density functional theory (QSDFT) model for slit/cylindrical pores (adsorption branch; N_2 at 77 K on carbon).

A Quanta 650 field-emission scanning electron microscope operating at 3 kV and a JEOL-2100 transmission electron microscope operating at 80 kV were used to characterize the morphology of the synthesized materials. For SEM characterization, the samples were prepared by adhesion of the sample directly on a conductive double-sided copper tape attached to SEM pin stub. For TEM characterization, the samples were dispersed in 2-propanol and a 3 µL of the dispersion were deposited onto a copper grid with Formvar/carbon layer. Samples were left at room temperature until dry.

Magnetization was studied with a vibrating sample magnetometer (MPMS-SQUID-VSM, LOT-Oriel) working at room temperature. The samples were prepared by placing around 5 mg of sample into gelatin capsules. The capsules were closed with a small piece of cotton and the sample compressed gently with a glass rod.

A microtiter plate reader model Synergy H1 from Biotek was used for fluorescence detection and quantification of OA and DTX-1 operating at 37 °C (excitation wavelength 315 nm, emission wavelength 470 nm).

3. *o*-Phthaldialdehyde (OPA) assay

Borate buffer solution (50 mM) at pH 9.0 was used as reaction buffer. 2-Mercaptoethanol at a concentration of 5 µL mL^{-1} in ethanol and *o*-phthaldialdehyde (OPA) at 10 mg mL^{-1} in ethanol were prepared. OPA solution must be protected from light. A series of standard amine solutions ranging from 0.03 mM to 0.53 mM were prepared by dilution of a butylamine stock solution (5 mM in ultrapure water) with ultrapure water. These standards were used to obtain a calibration curve by plotting the obtained fluorescence intensity versus the concentration of $–NH_2$ groups in mmol. For the Fe_3O_4@DOPA or Fe_3O_4@DOPA-Tp samples, around 3 mg of the material were dispersed in ultrapure water by ultrasonication for 10 min.

To prepare the OPA reagent, 883 µL of borate buffer solution, 83 µL of 2-mercaptoethanol (5 µL mL^{-1} in ethanol), and 34 µL of OPA (10 mg mL^{-1} in ethanol) were mixed and left standing for 2 h at room temperature in the dark. Afterwards, 34 µL of the sample were added and the fluorescence was recorded 1 min after addition. Excitation wavelength was set at 336 nm; emission at 450 nm.

The concentration of $–NH_2$ groups in the sample was determined by interpolation of the calibration curve.

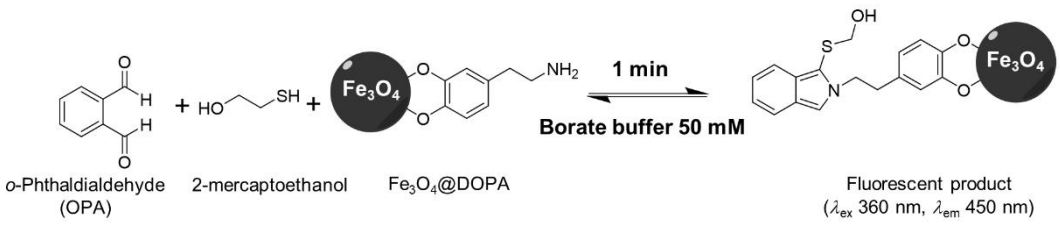

Scheme S3.1. Reaction of OPA with amines to form a fluorescent product.

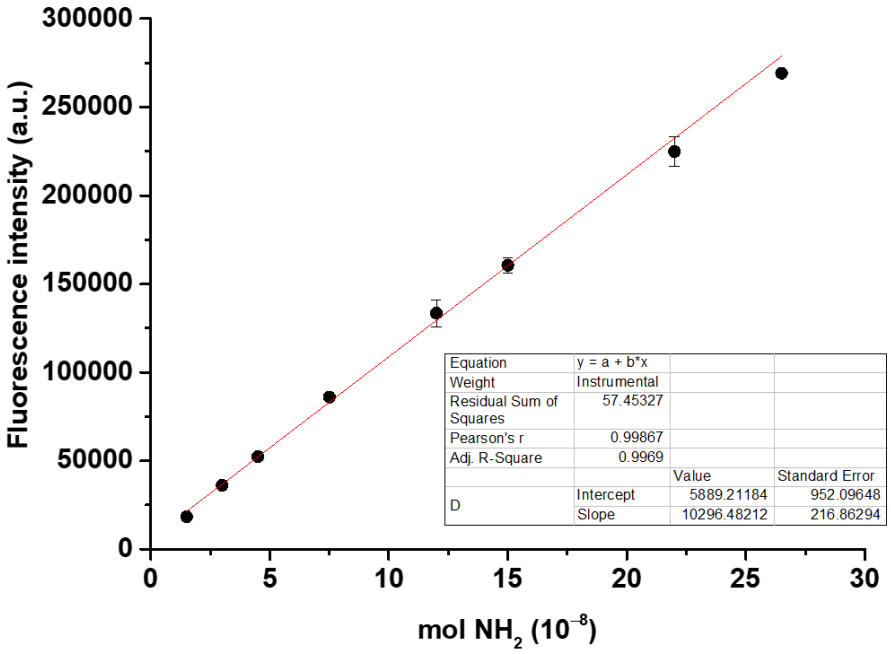

Figure S3.1. Calibration curve for OPA assay using butylamine as standard.

Table S3.1. Quantification of available $–NH_2$ moieties on the synthesized Fe_3O_4@DOPA from three different batches.

Batch	mg of Fe_3O_4@DOPA used for OPA assay	mmol $–NH_2$	mmol $–NH_2$ g^{-1} NPs
1	3.3	0.00041	0.125
2	3.8	0.00039	0.102
3	3.1	0.00035	0.112

Calculation of not polymerized dopamine (%) in the synthesized Fe_3O_4@DOPA NPs

TGA analysis of Fe_3O_4@DOPA NPs showed an organic content of around 15% attributed to the DOPA layer. Taking into account that 16 mg of Fe_3O_4@DOPA NPs were used for TGA analysis, we can estimate that 2.5 mg correspond to the organic coating. Assuming that the organic coating is all as dopamine (MW = 153.18 g mol^{-1}) we can estimate the amount of free NH_2 groups as 0.017 mmol.

On the other hand, quantification of free primary amino groups (OPA assay, see above) gave a content of 0.125 mmol of NH_2 per gram of NPs. Taking into account that 6.7 mg of Fe_3O_4@DOPA NPs were used for OPA assay, we can calculate the experimental amount of NH_2 as 0.00083 mmol of NH_2.

- Calculated free NH_2 (mmol) from TGA = 0.017 mmol
- Experimental free NH_2 (mmol) from OPA assay = 0.00083 mmol

$$\frac{0.00083\ mmol\ NH_2}{0.017\ mmol\ NH_2} \times 100 \cong 5\ \%\ DOPA$$

4. Experimental conditions for the synthesis of mTpBD-Me_2

Table S4.1 Experimental conditions for the synthesis of mTpBD-Me_2.

Name / Reagents	0.005-mTpBD-Me_2	0.025-mTpBD-Me_2	0.05-mTpBD-Me_2	0.1-mTpBD-Me_2	0.2-mTpBD-Me_2	0.4-mTpBD-Me_2
Tp, mg [mmol]	1 [0.005]	2 [0.025]	10.5 [0.05]	21 [0.1]	42 [0.2]	84 [0.4]
***o*-Tolidine, mg [mmol]**	1.6 [0.075]	8 [0.038]	16 [0.075]	32 [0.15]	64 [0.3]	127 [0.6]
Aq. acetic acid 6 M, µL	3	15	30	60	120	233

Molar ratio: Tp/*o*-tolidine 1:1.5; Tp/acetic acid 1:3.5;
Fe_3O_4@DOPA-Tp (25 mg mL^{-1}) dispersed in dioxane: 2 mL;
Anhydrous dioxane: 3 mL

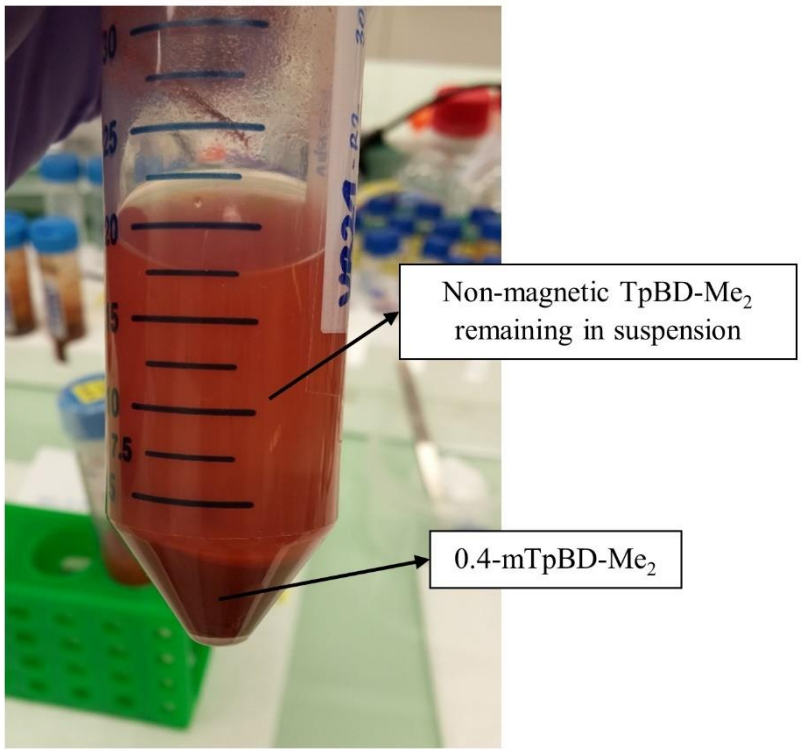

Figure S4.1. Image of the reaction medium after synthesis of 0.4-mTpBD-Me_2 using Tp amount of 80 mmol.

5. Thermogravimetric analyses (TGA)

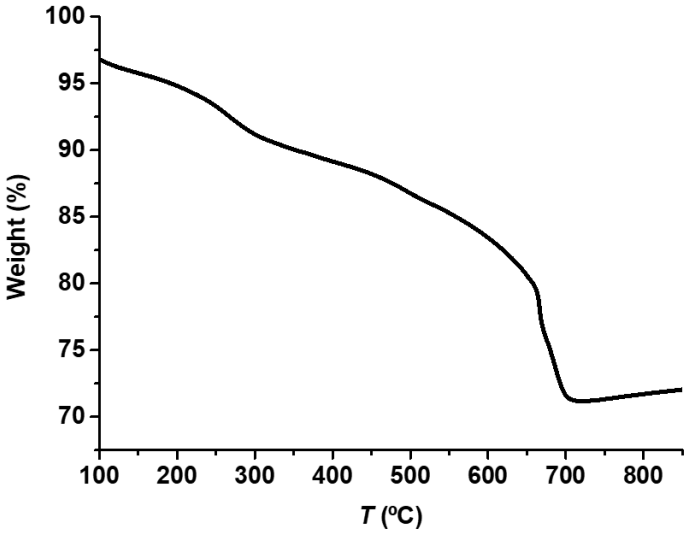

Figure S5.1. TGA data of Fe_3O_4@DOPA.

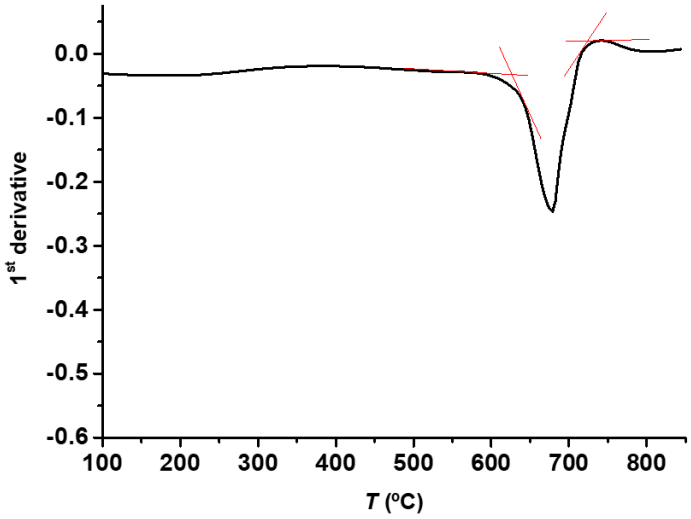

Figure S5.2. 1st Derivative of the TGA data of Fe_3O_4@DOPA.

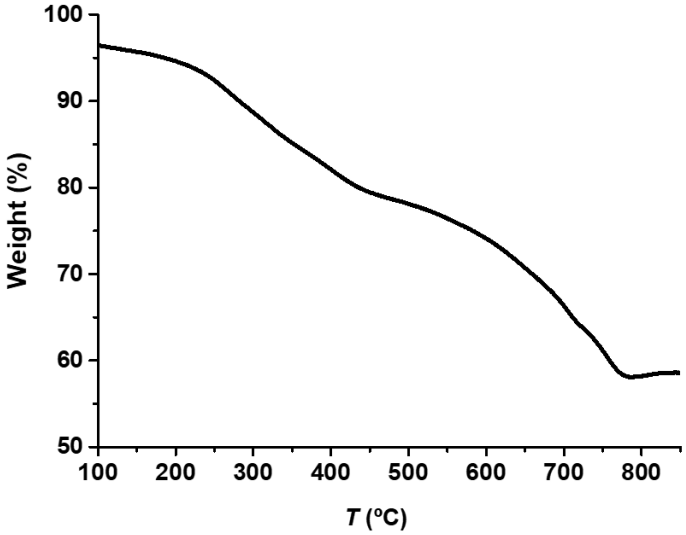

Figure S5.3. TGA data of Fe_3O_4@DOPA-Tp.

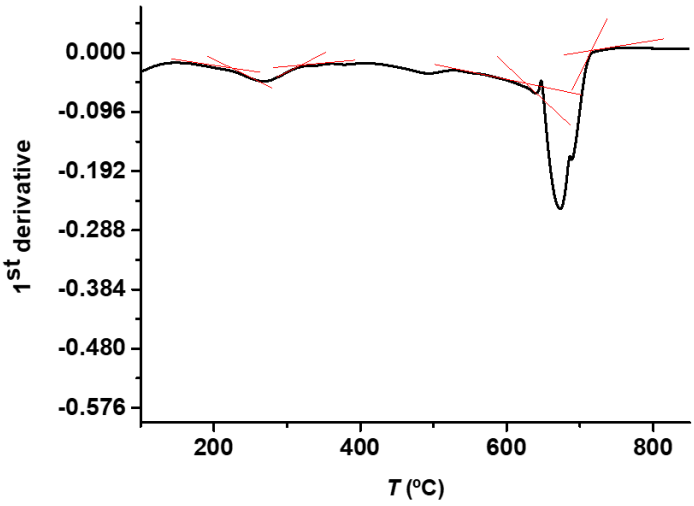

Figure S5.4. 1st Derivative of the TGA data of Fe_3O_4@DOPA-Tp.

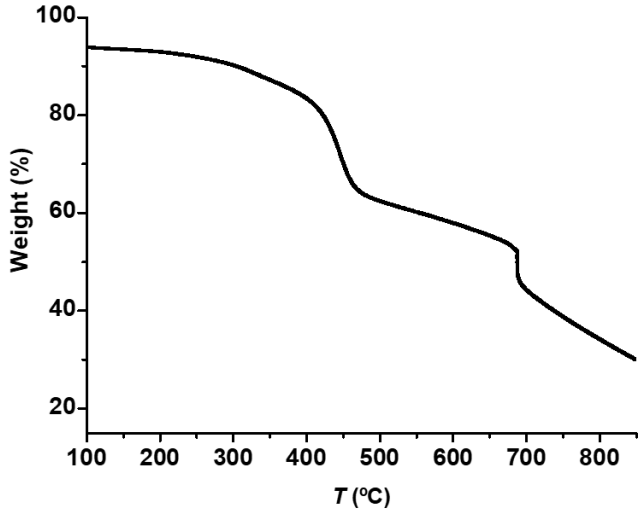

Figure S5.5. TGA data of 0.2-mTpBD-Me_2.

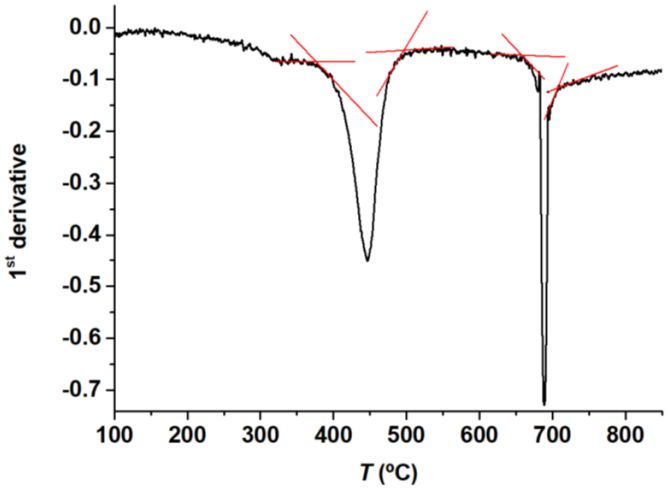

Figure S5.6. 1st derivative TGA data of 0.2-mTpBD-Me_2.

6. Fourier-transform infrared (FT-IR)

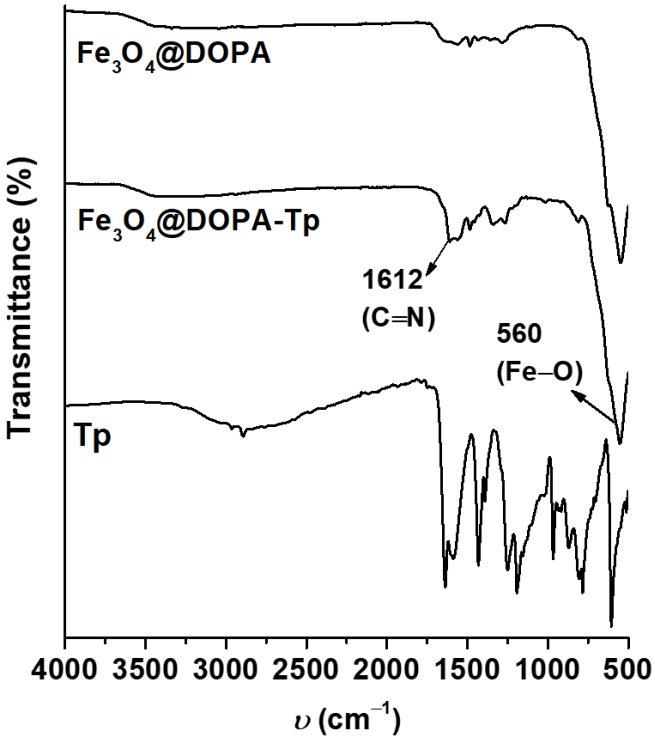

Figure S6.1. FT-IR spectrum of FT-IR spectra of Fe_3O_4@DOPA, Fe_3O_4@DOPA-Tp, and Tp.

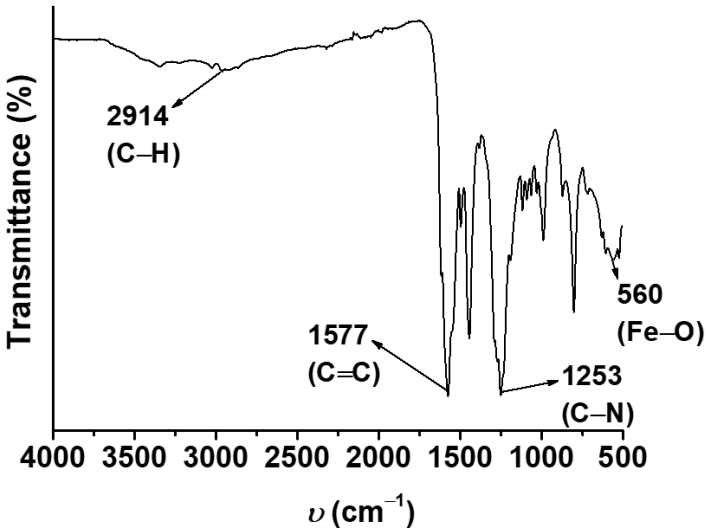

Figure S6.2. FT-IR spectrum of 0.2-mTpBD-Me_2.

7. Small angle X-ray scattering (SAXS)

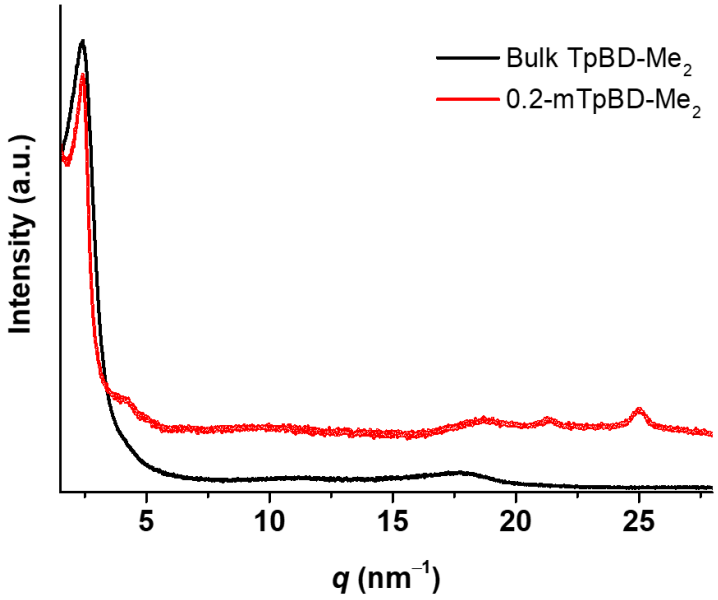

Figure S7.1. SAXS patterns of bulk TpBD-Me_2 (black) and 0.2-mTpBD-Me_2 (red).

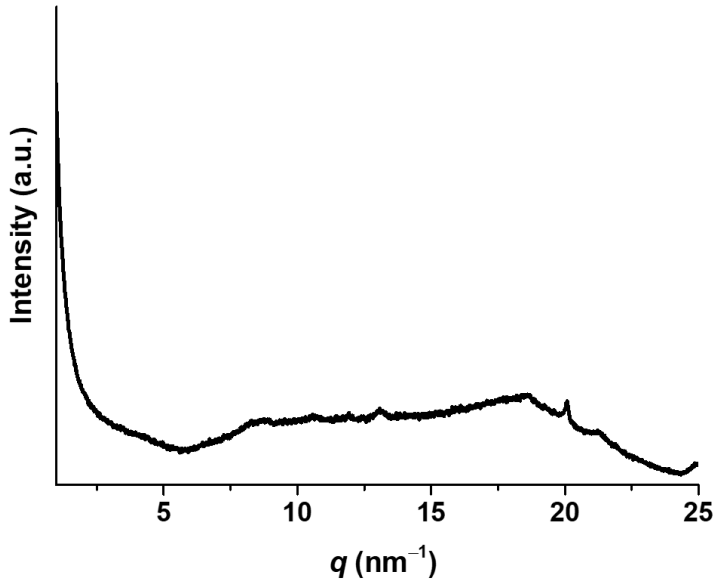

Figure S7.2. SAXS pattern of the obtained product using conditions of 0.2-mTpBD-Me_2 with non-pre-functionalized Fe_3O_4@DOPA nanoparticles as substrate.

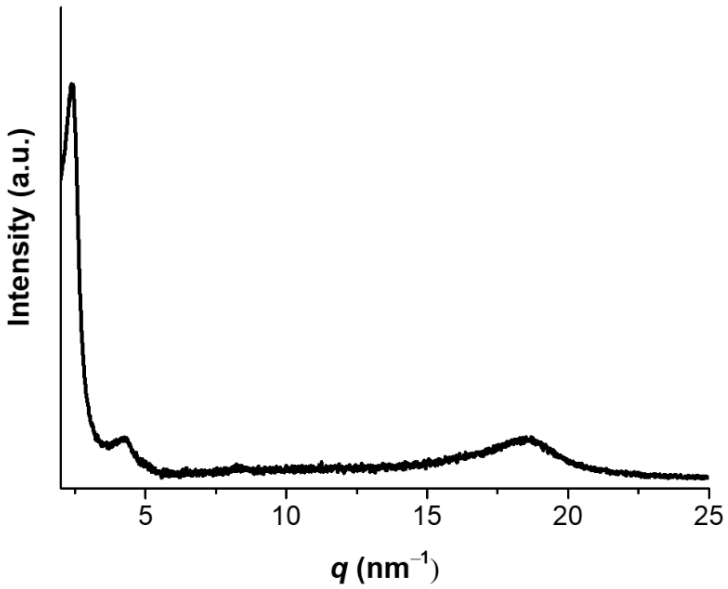

Figure S7.3. SAXS pattern of the non-magnetic phase from the synthesis of 0.4-mTpBD-Me_2 corresponding to TpBD-Me_2.

8. X-Ray diffraction (XRD)

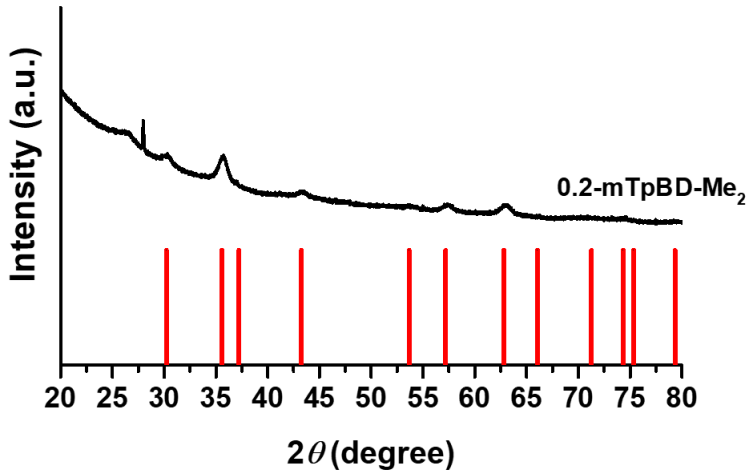

Figure S8.1. XRD pattern of 0.2-mTpBD-Me_2 (red lines correspond to the magnetite standard pattern JCPDS 19-0629).

9. N_2 physisorption

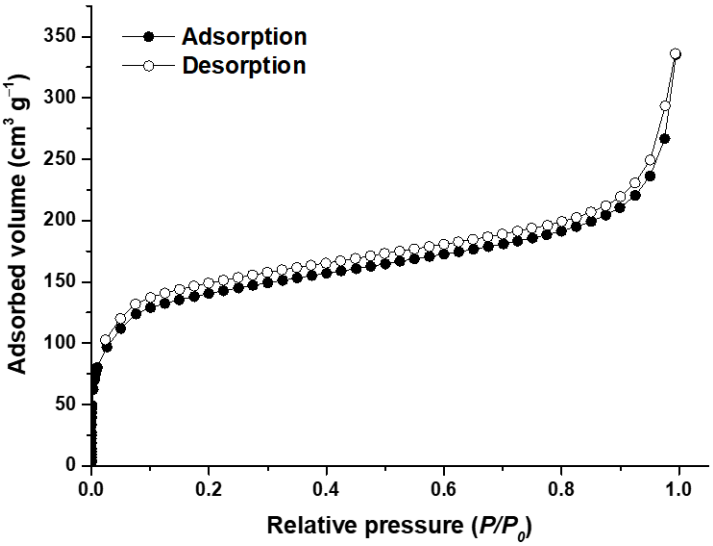

Figure S9.1. Nitrogen adsorption (filled circles) and desorption (hollow circles) isotherms of 0.1-mTpBD-Me_2 measured at 77 K.

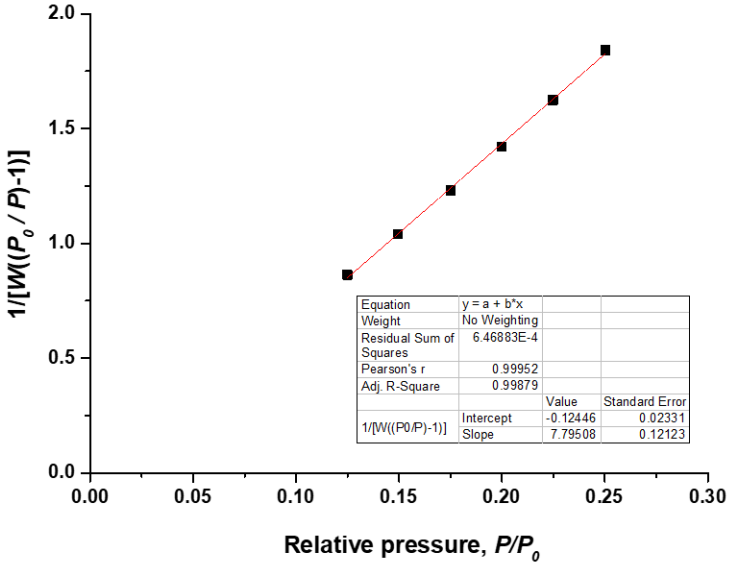

Figure S9.2. Multi-point BET plot and linear fit of 0.1-mTpBD-Me_2.

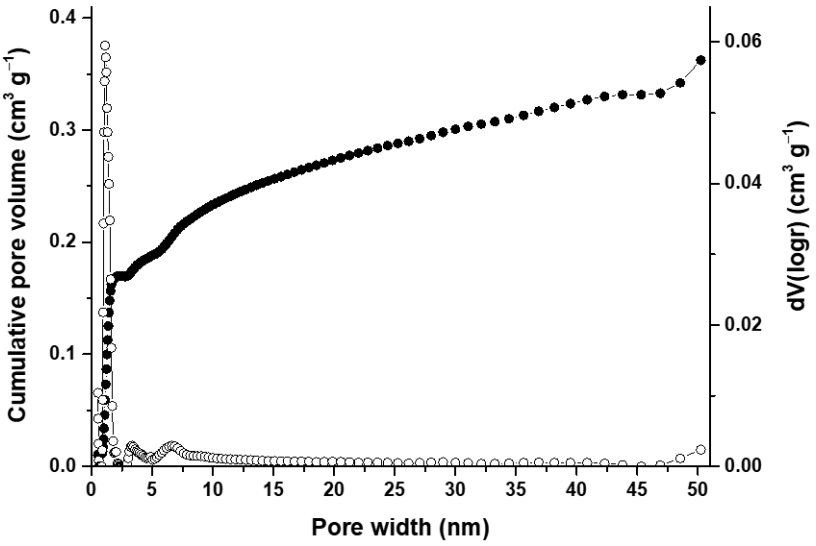

Figure S9.3. Pore size distribution (hollow circles) and cumulative pore volume (filled circles) profiles of 0.1-mTpBD-Me_2.

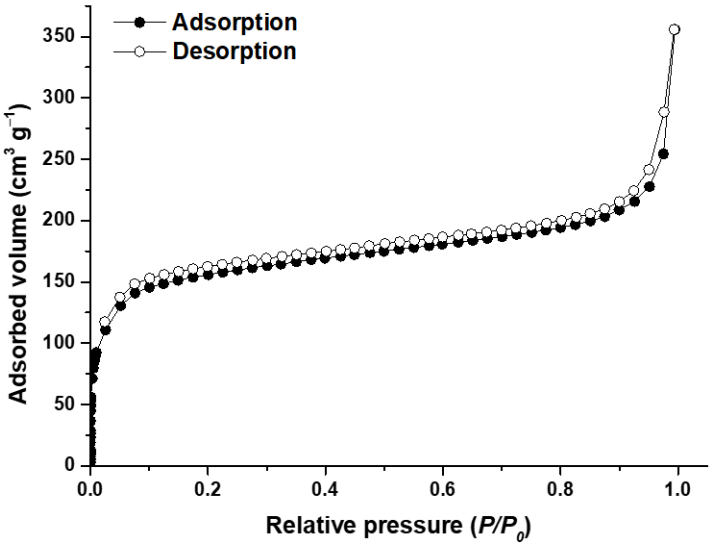

Figure S9.4. Nitrogen adsorption (filled circles) and desorption (hollow circles) isotherms of 0.4-mTpBD-Me_2 measured at 77 K.

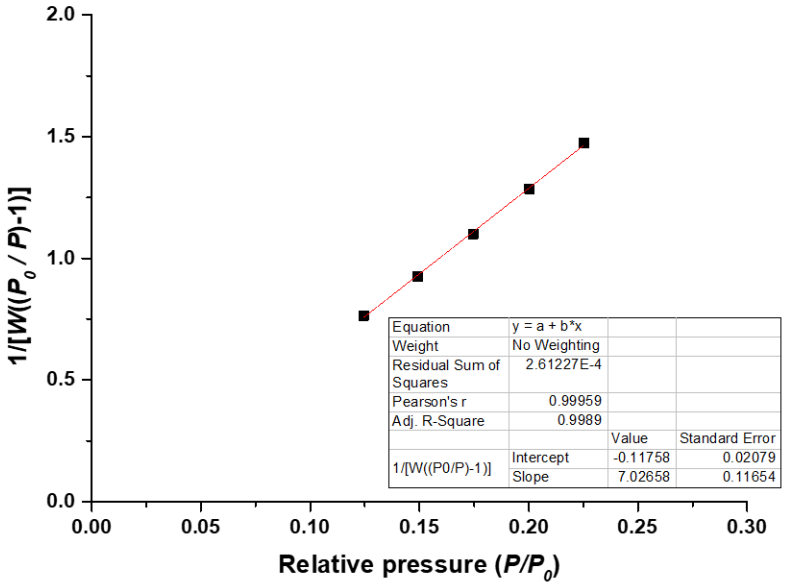

Figure S9.5. Multi-point BET plot and linear fit of 0.4-mTpBD-Me_2.

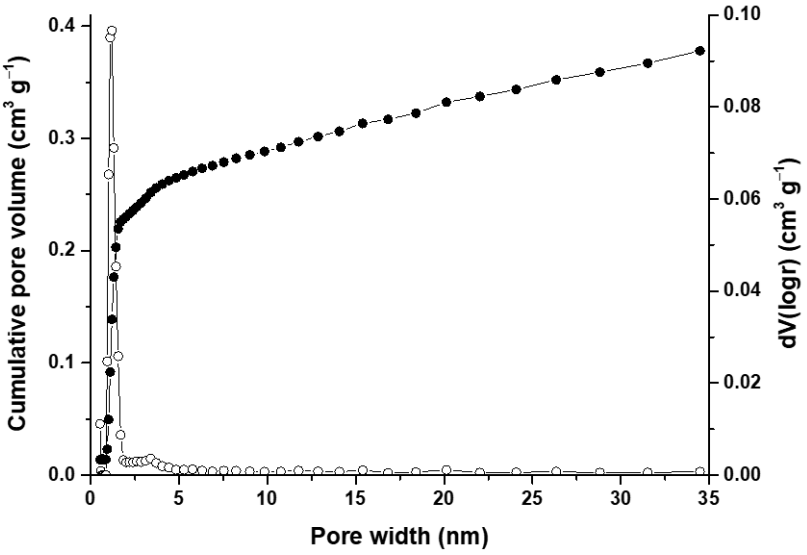

Figure S9.6. Pore size distribution (hollow circles) and cumulative pore volume (filled circles) profiles of 0.4-mTpBD-Me_2.

10. Magnetic measurements

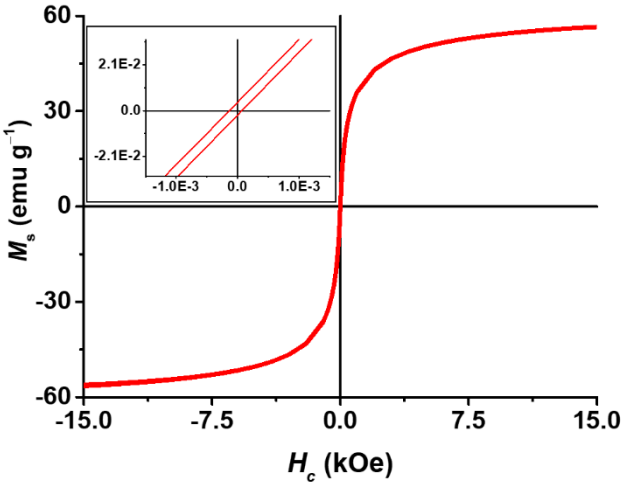

Figure S10.1. Hysteresis loop of Fe_3O_4@DOPA-Tp

Table S10.1. Saturation magnetization (M_s) and coercive force (H_c) of synthesized Fe_3O_4@DOPA, Fe_3O_4@DOPA-Tp, and mTpBD-Me_2.

Sample	M_s (emu g^{-1})	H_c (Oe)
Fe_3O_4@DOPA	60.5	0.005
Fe_3O_4@DOPA-Tp	61.3	0.060
0.1-mTpBD-Me_2	13.5	0.100
0.2-mTpBD-Me_2	9.90	0.150
0.4-mTpBD-Me_2	4.90	0.330

11. Scanning electron microscopy (SEM)

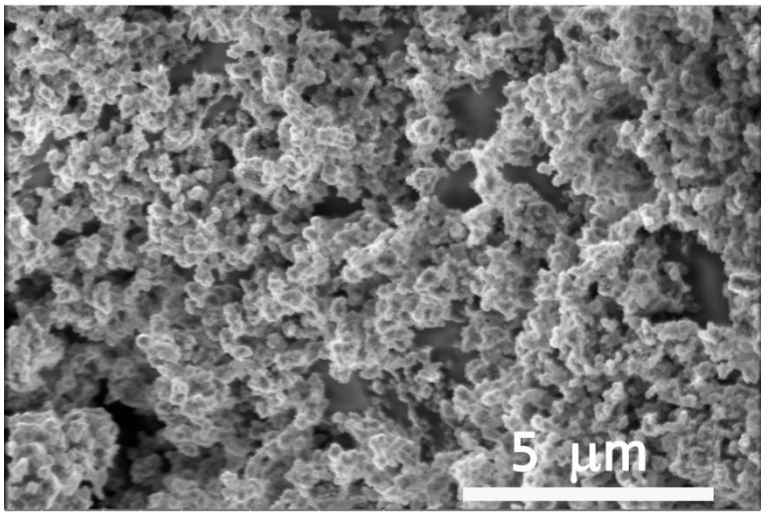

Figure S11.1. SEM image of 0.2-mTpBD-Me_2

12. Transmission electron microscopy (TEM) and energy-dispersive X-ray spectroscopy (EDX) analysis

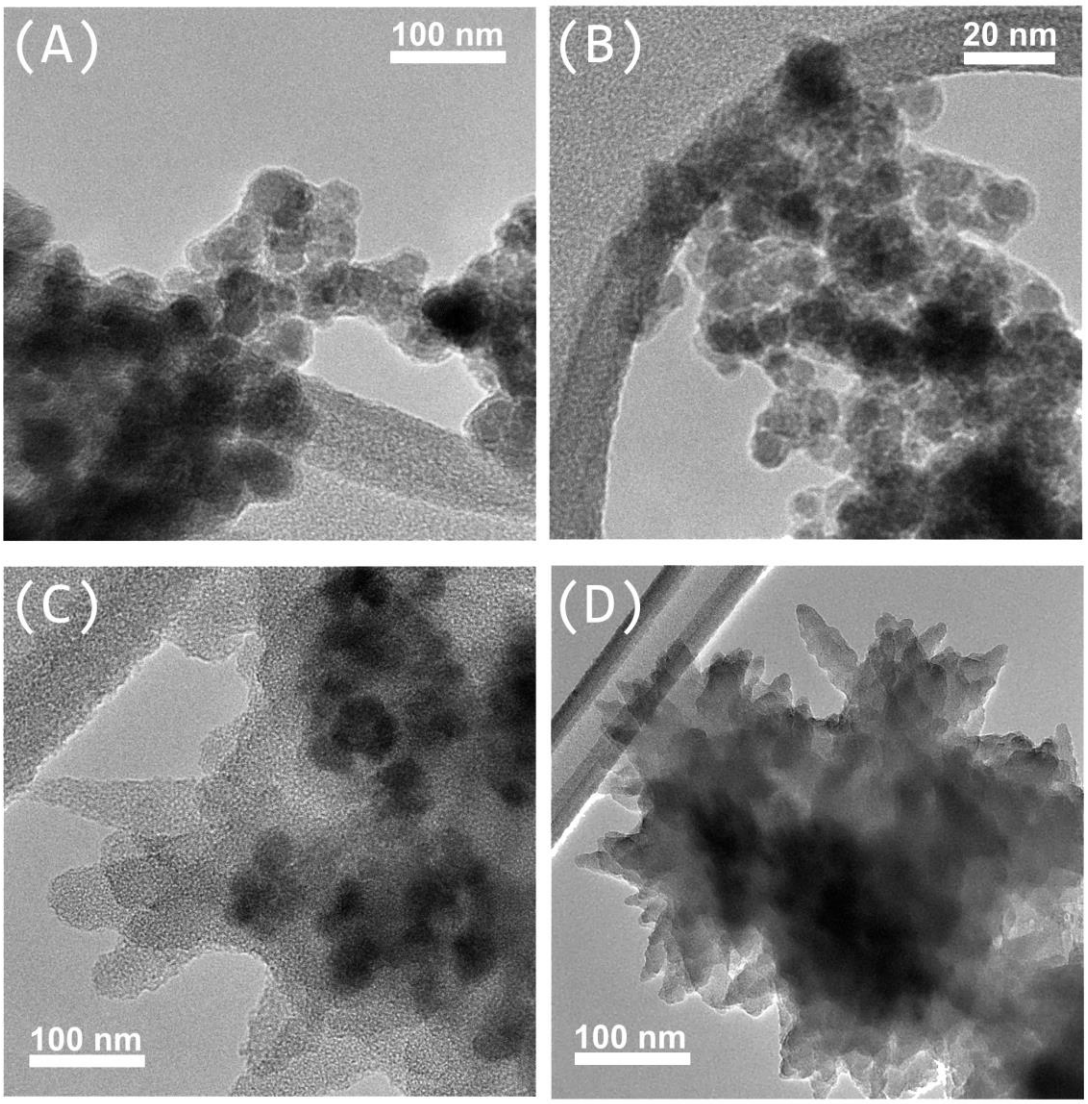

Figure S12.1. TEM characterization of mTpBD-Me_2: (A) 0.005-mTpBD-Me_2, (B) 0.025-mTpBD-Me_2, (C) 0.1-mTpBD-Me_2, and (D) 0.4-mTpBD-Me_2. The TEM sequence shows that the COF shell (lighter shell) grows progressively around Fe_3O_4 aggregates (dark spots). Inset in B shows the TEM micrograph with high magnification.

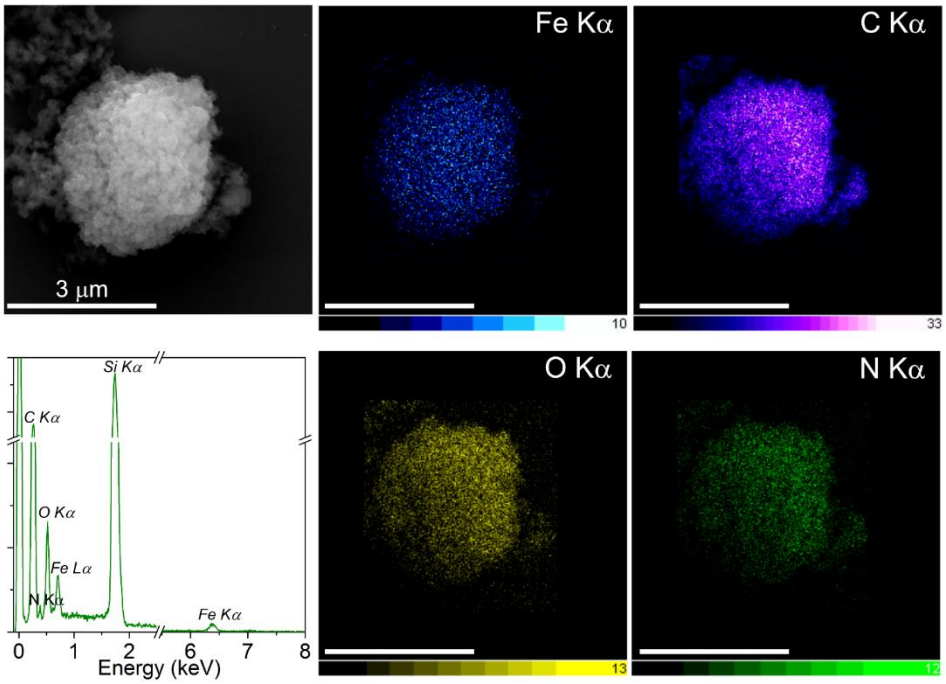

Figure S12.2. EDX analysis of crystalline 0.2-mTpBD-Me_2 confirming the presence of both materials (Fe_3O_4 and TpBD-Me_2) in the synthesized composite.

13. Adsorption and desorption of OA and DTX-1

OA and DTX-1 quantification

Reaction buffer consisted of 20 mM Tris-HCl, 5 mM $MgCl_2$, 1 mM $MnCl_2$, 1 mg mL^{-1} bovine serum albumin (BSA), and 0.1% 2-mercaptoethanol at pH = 8. DiFMUP stock solution was prepared at 40 mM in Tris-HCl solution. Biotoxin stock solutions (OA and DTX-1 reconstituted from the lyophilized product) were prepared at 1 mM in absolute ethanol for OA and methanol for DTX-1. A stock solution of PP1 at 3900 U mL^{-1} was prepared by reconstitution of the lyophilized product with ultrapure water. Separated calibration curves were used for each quantification experiment of OA and DTX-1 measured in the same microplate with the rest of the samples. OA and DTX-1 standard solutions for the calibration curves were prepared in the corresponding solvent, synthetic seawater for the quantification from the adsorption assays and 2-propanol or 70% ethanol for the quantification of the supernatant from the desorption assays. For the calibration curves, PP1 inhibition assays were performed at a final volume of 200 µL in wells of flat-bottom opaque 96-well microplates. Briefly, first, 10 µL of 0.1 U of PP1 (intermediate solution prepared by dilution of the stock with Tris-HCl solution) were added to the reaction wells containing 165 µL of reaction buffer. Then, 20 µL of the corresponding solution of the biotoxin calibration curve, solvent (blank), or supernatant samples from the adsorption/desorption assays were added to the well. After that, the microplate was incubated during 30 min under constant shaking at 500 rpm at 37 °C for a maximum enzymatic inhibition. Then, 5 µL of 8 mM DiFMUP solution (prepared by dilution of the stock with Tris-HCl solution) was added. After 2 h under constant shaking at 500 rpm at 37 °C, fluorescence intensity was measured (excitation wavelength 315 nm, emission wavelength 470 nm) in a BioTek Synergy H1 microplate reader. Analytical determinations were carried out in duplicate.

Preparation of 0.2-mTpBD-Me_2 suspensions for MSPE of OA and DTX-1

Table S13.1. Amount of 0.2-mTpBD-Me_2 dispersed in 100 µL of synthetic seawater to perform MSPE of OA and DTX-1.

Composite	Organic content from TGA (%)	Amount dispersed (mg)
0.2-mTpBD-Me_2	84	1.25

Calibration curves for OA and DTX-1 quantification

Calibration curves were made using the software Origin9® by plotting known concentrations of serial dilutions against their respective fluorescence read at 470 nm. Then, a non-linear pharmacology dose-response fitting was applied. Calibration curves were made using synthetic seawater or 2-propanol as solvent for calibration standard dilutions. Below are exemplary calibration curves made for each biotoxin with the used solvents. The calibration curve for each solvent represents the average fluorescent values from three different experiments. The error bars were calculated as standard deviation (SD).

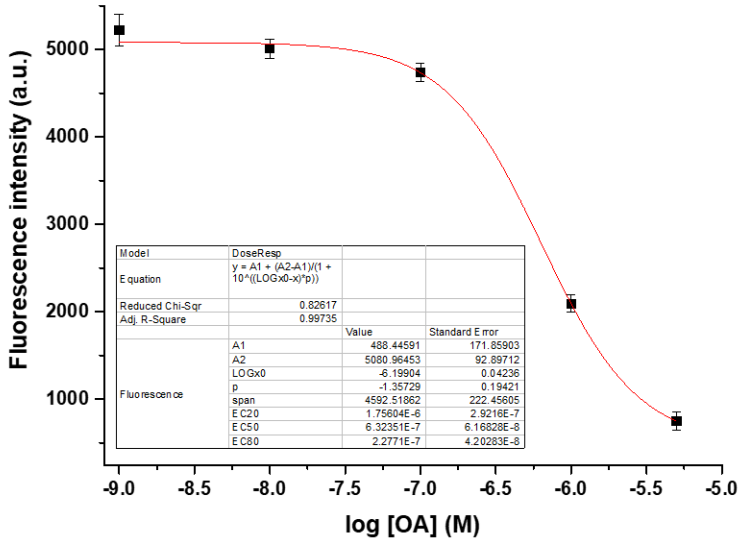

Figure S13.1. OA calibration curve in synthetic seawater.

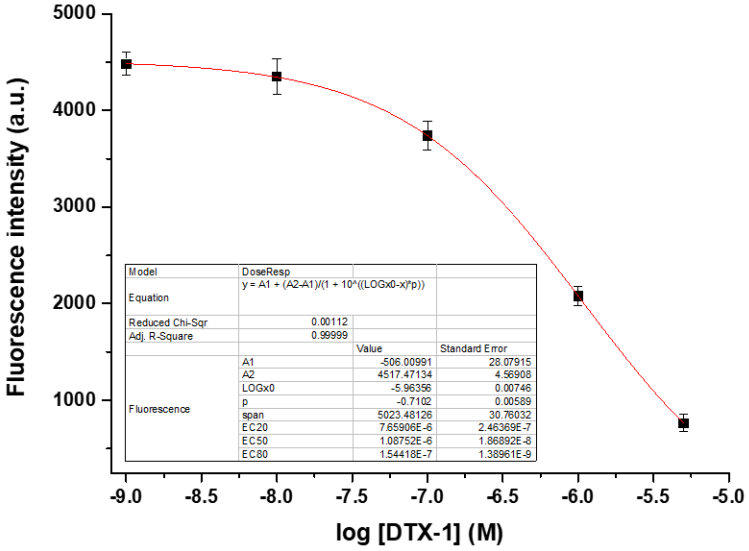

Model	DoseResp		
Equation	y = A1 + (A2-A1)/(1 + 10^((LOGx0-x)*p))		
Reduced Chi-Sqr	0.00112		
Adj. R-Square	0.99999		
		Value	Standard Error
Fluorescence	A1	-506.00991	28.07915
	A2	4517.47134	4.56908
	LOGx0	-5.96356	0.00746
	p	-0.7102	0.00589
	span	5023.48126	30.76032
	EC20	7.65906E-6	2.46369E-7
	EC50	1.08752E-6	1.86892E-8
	EC80	1.54418E-7	1.38961E-9

Figure S13.2. DTX-1 calibration curve in synthetic seawater.

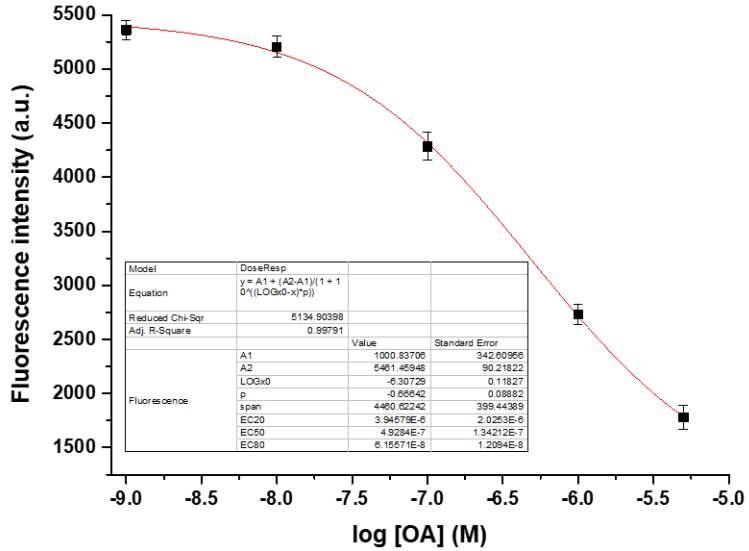

Model	DoseResp		
Equation	y = A1 + (A2-A1)/(1 + 10^((LOGx0-x)*p))		
Reduced Chi-Sqr	5134.90398		
Adj. R-Square	0.99791		
		Value	Standard Error
Fluorescence	A1	1000.83706	342.60956
	A2	5461.45948	90.21822
	LOGx0	-6.30729	0.11827
	p	-0.66642	0.08882
	span	4460.62242	399.44389
	EC20	3.94579E-6	2.0253E-6
	EC50	4.9284E-7	1.34212E-7
	EC80	6.15571E-8	1.2094E-8

Figure S13.3. OA calibration curve in 2-propanol.

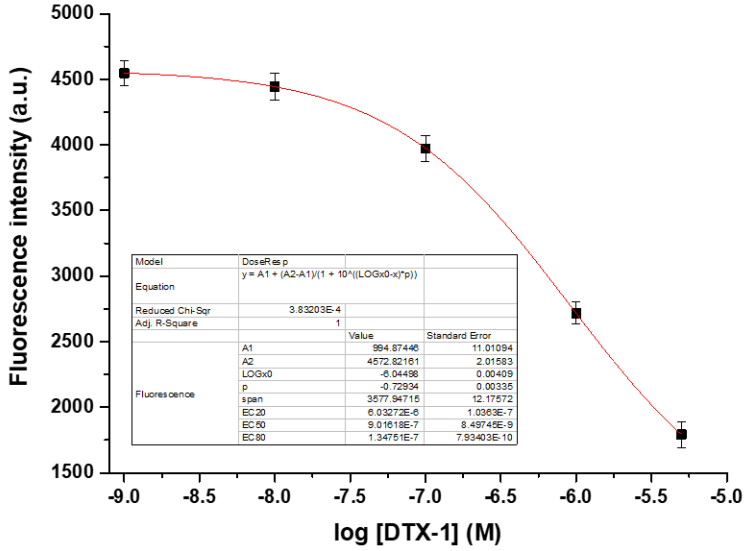

Figure S13.4. DTX-1 calibration curve in 2-propanol.

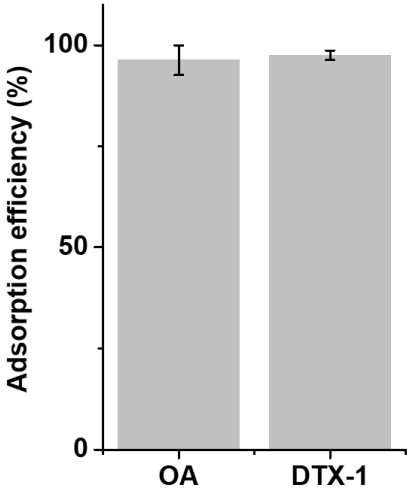

Figure S13.5. OA and DTX-1 adsorption efficiency (%) with 0.2-mTpBD-Me_2. Samples of 100 µL of mTpBD-Me_2 composite dispersion in synthetic seawater at 1 mg mL^{-1} COF were spiked with an OA or DTX-1 concentration of 10 µmol L^{-1}, and incubated at 19 °C under constant shaking at 1500 rpm during 120 min. After incubation, the samples were collected by an external magnetic field (10 min). Supernatants were collected and quantified for either OA or DTX-1.

Adsorption kinetics

Samples of 100 µL of 0.2-mTpBD-Me_2 dispersed in synthetic seawater at 1 mg mL^{-1} COF were spiked with OA or DTX-1 concentration of 10, 15, 50, or 100 µmol L^{-1}, and incubated at 19 °C under constant shaking at 1500 rpm After 0.5, 60, 240, and 480 min of incubation, the sample for the corresponding time point was collected by an external magnetic field (10 min). Supernatants were collected and quantified for OA or DTX-1.

Two replicates for each concentration and each time were done. The time used for magnetic separation was added to the time points as time elapsed, resulting in time points of 10.5, 70, 250, and 490 min, respectively.

Desorption kinetics

Samples of 100 µL of 0.2-mTpBD-Me_2 dispersed in synthetic seawater at 1 mg mL^{-1} COF were spiked with OA or DTX-1 concentration of 10, 15, 50, or 100 µmol L^{-1}, and incubated at 19 °C under constant shaking at 1500 rpm for 120 min. After incubation, the 0.2-mTpBD-Me_2 composite was separated by applying an external magnetic field for 10 min. The supernatants were collected for quantification of non-adsorbed biotoxin. Before desorption, 0.2-mTpBD-Me_2 was washed with ultrapure water (200 µL, incubation 15 min, 19 °C, 1500 rpm). Then, desorption kinetics were carried out by adding 200 µL of 2-propanol and incubating during 1, 60, 240, or 480 min at 19 °C under constant shaking at 1500 rpm. The solid phase was then collected with an external magnet in 5 min. Supernatants were recovered and analyzed for OA or DTX-1.

Two replicates for each concentration and each time were done. The time used for magnetic separation was added to the time points as time elapsed, resulting in time points of 6, 65, 245, and 485 min, respectively.

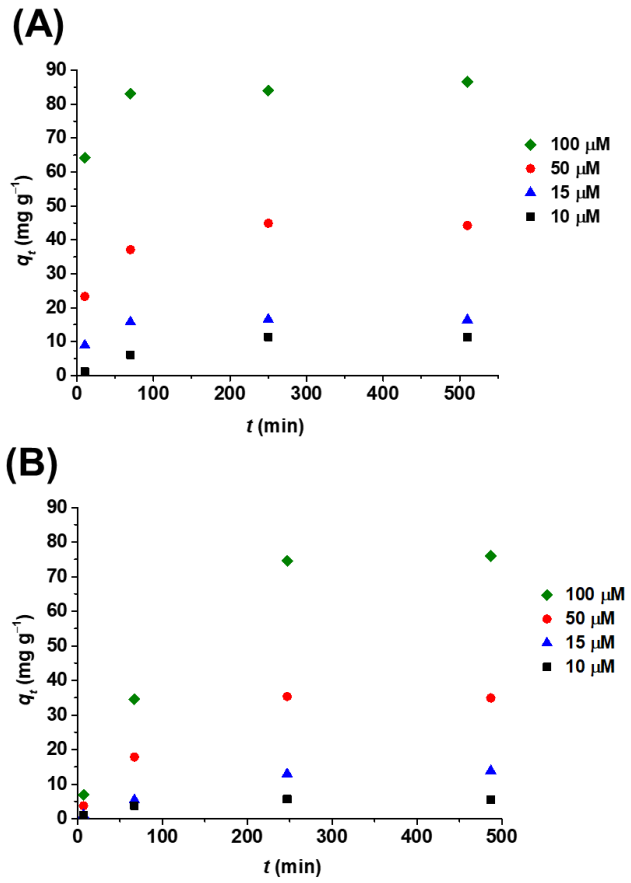

Figure S13.6. (A) DTX-1 adsorption kinetic curve of 0.2-mTpBD-Me_2 with initial concentrations of 10, 15, 50, and 100 μmol L^{-1} in seawater at 19 °C; (B) DTX-1 desorption kinetic curve of 0.2-mTpBD-Me_2 with initial concentrations of 10, 15, 50, and 100 μmol L^{-1} in 2-propanol at 19 °C.

Isotherms at 19 °C

Freundlich equation was used to analyze the equilibrium adsorption isotherm. Freundlich equation is expressed as:[1]

$$\log q_e = \log K_F + \left(\frac{1}{n}\right) \times \log C_e$$

where q_e is the adsorbate concentration on the adsorbent in equilibrium (mg g^{-1}), C_e is the equilibrium concentration of adsorbate in solution (mg L^{-1}), and n and K_F are characteristic constants. K_F is an indicator of the adsorption capacity in the Freundlich theory. This constant decreases with increasing temperature and is also related to the strength of adsorbate–sorbent interaction.

The maximum adsorption capacity (q_m) can be calculated from the following equation:

$$q_m = K_F \, C_0^{1/n}$$

where C_0 is the initial concentration of the adsorbate in solution (mg L^{-1}).

The Freundlich model showed a good fit to the experimental data in a moderate solute concentration range, and provides information about the heterogeneity of the surface of the adsorbent by means of 1/n value.

As shown in Table S13.2, the experimental data fitted well to Freundlich model. Furthermore, the constant n is higher than 1, indicating favorable adsorption and showing the homogeneity of the adsorbent surface. The linear tendency of the isotherm for OA and DTX-1 (Figure S13.6) indicates that the adsorbed amount is proportional to the equilibrium concentration of the solute in the solution. Scarcity and high cost of the OA and DTX-1 toxin standards prevented us from expanding the isotherm to higher concentrations to further confirm the applicability of the Freundlich model.

Table S13.2. Freundlich isotherm equation constants and correlation coefficient derived from the graph in Figures S13.6**.**

OA	
Regression equation	lg q_e = (0.781 ± 0.064)lg C_e + (1.421 ± 0.040)
K_F ($mg^{1-1/n}$ g^{-1} $L^{1/n}$)	26.363 ± 1.095
1/*n*	0.781 ± 0.064
n	1.280
R^2	0.9676
DTX-1	
Regression equation	lg q_e = (0.819 ± 0.080)lg C_e + (1.352 ± 0.041)
K_F ($mg^{1-1/n}$ g^{-1} $L^{1/n}$)	22.508 ± 1.101
1/*n*	0.819 ± 0.080
n	1.221
R^2	0.9537

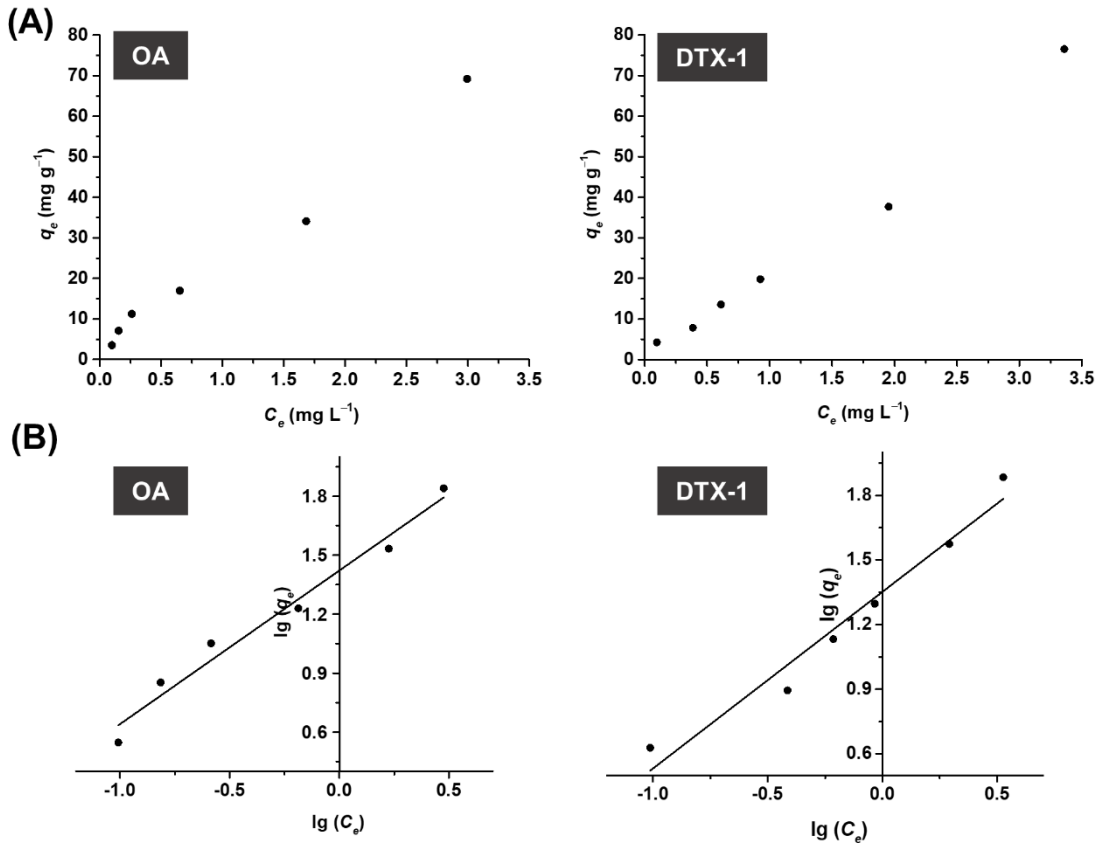

Figure S13.7. (A) Amount of biotoxin adsorbed in equilibrium (120 min), q_e (mg g^{-1}), as a function of biotoxin concentration in equilibrium, C_e (mg L^{-1}); (B) linear regression of the Freundlich isotherm for the experimental adsorption of OA and DTX-1 by 0.2-mTpBD-Me_2 composite.

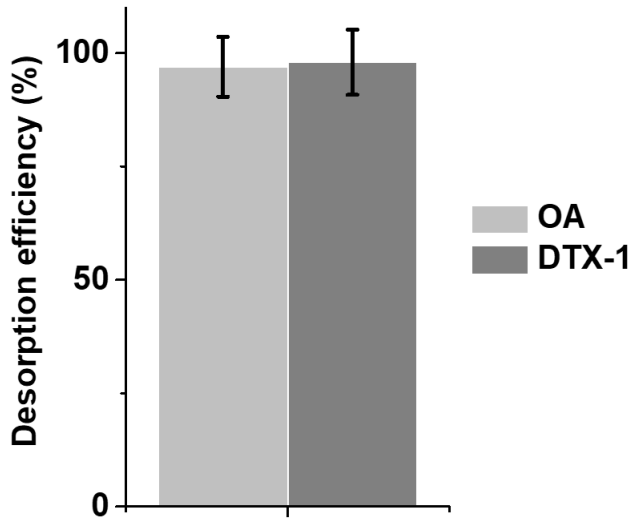

Figure S13.8. Quantification of the desorption efficiency (%) from 0.2-mTpBD-Me_2 using 2-propanol at 19 °C (240 min) as solvent after adsorption assays with 10 µM of OA or DTX-1.

Table S13.3. Comparison with styrene-based commercial resins SPATTs tested for OA and DTX-1 adsorption from spiked seawater samples. It is clear from the table that despite the lower adsorbent amount and shorter treatment time used with the COF-based 0.2-mTpBD-Me_2 adsorbent, higher adsorption efficiency of both biotoxins is reached.

Adsorbent	Surface area ($m^2\ g^{-1}$)	Adsorbate	[Adsorbate] µM	Adsorption efficiency (%)	Amount of sorbent ($mg\ mL^{-1}$)	Extraction conditions (h, °C)	Ref
L-493	1100	OA	0.15	15.5	12	72, 6	2
		DTX-1	0.12	16.9	12	72, 6	
HP-20	588	OA	0.15	31.6	12	72, 6	2
			4.5	70	300	24, n/a	3
		DTX-1	0.12	25.4	12	72, 6	2
SP825	1000	OA	0.15	19.5	12	72, 6	2
		DTX-1	0.12	19.0	12	72, 6	
SP850	1000	OA	0.15	18.4	12	72, 6	2
		DTX-1	0.12	19.3	12	72, 6	
XAD-4	725	OA	0.15	16.9	12	72, 6	2
		DTX-1	0.12	19.1	12	72, 6	
Strata-X	800	OA	4.5	80	300	24, n/a	3
Oasis HLB	800	OA	4.5	52	300	24, n/a	3
0.2-mTpBD-Me_2	538	OA	10	94	1	2, 19	This work
		DTX-1	10	98	1	2, 19	

14. Recycling

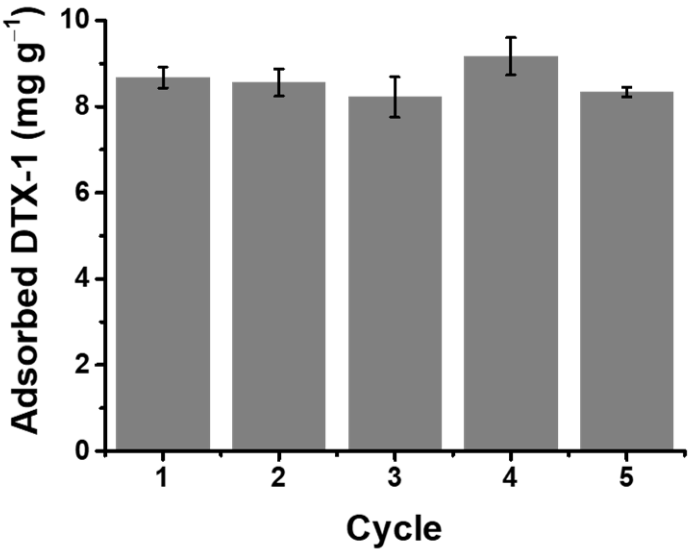

Figure S14.1. Reusability of 0.2-mTpBD-Me_2 in five consecutive adsorption/desorption cycles of DTX-1 with a concentration of biotoxin 10 µM in synthetic seawater at 19 °C. Synthetic seawater was used as matrix for adsorption (19 °C, 2 h, 1400 rpm) and 2-propanol was used as solvent for desorption (19 °C, 4 h, 1400 rpm).

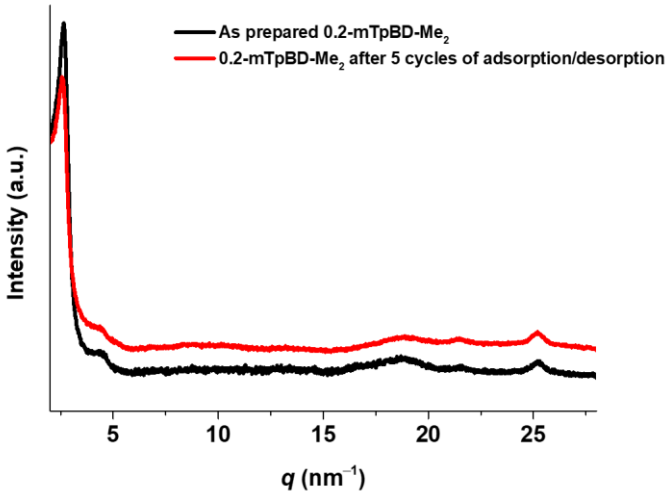

Figure S14.2. A comparison of the SAXS data of 0.2-mTpBD-Me_2 as prepared (black) and after five cycles of adsorption/desorption without spiking with biotoxins (red). To mimic the conditions of adsorption/desorption of biotoxins, five cycles were carried out with 18 mg of 0.2-mTpBD-Me_2 dispersed in 15 mL of synthetic seawater for adsorption and 30 mL of 2-propanol for desorption.

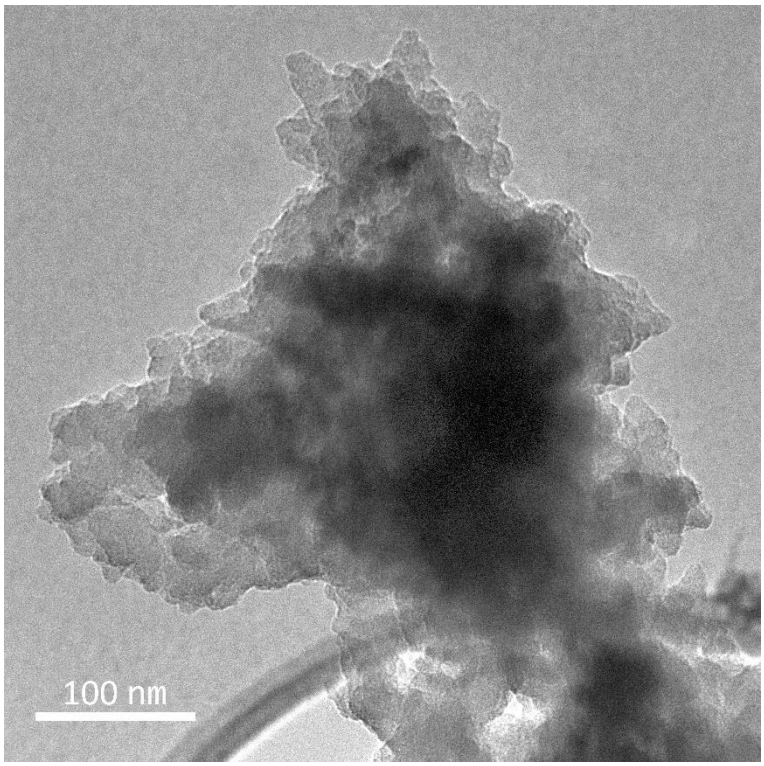

Figure S14.3. TEM characterization of 0.2-mTpBD-Me_2 after five cycles of adsorption/desorption.

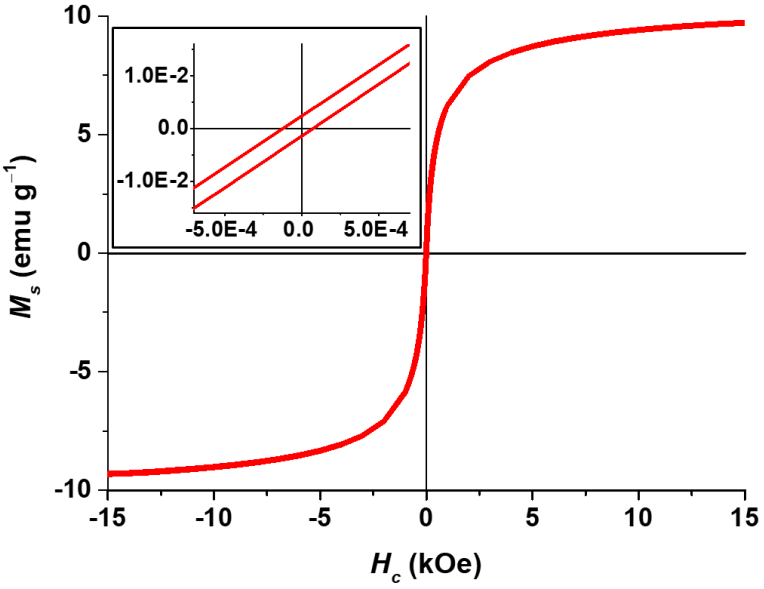

Figure S14.4. Hysteresis loop of 0.2-mTpBD-Me_2 after five cycles of adsorption/desorption.

15. Biotoxin structures

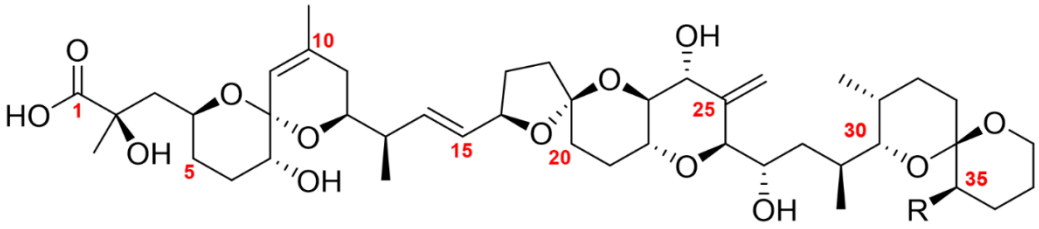

	R
Okadaic acid (OA)	**–H**
DTX-1	**–CH_3**

Figure S15.1. The chemical structures of OA and DTX-1.

16. Magnetic separation of 0.2-mTpBD-Me_2 from seawater and 2-propanol

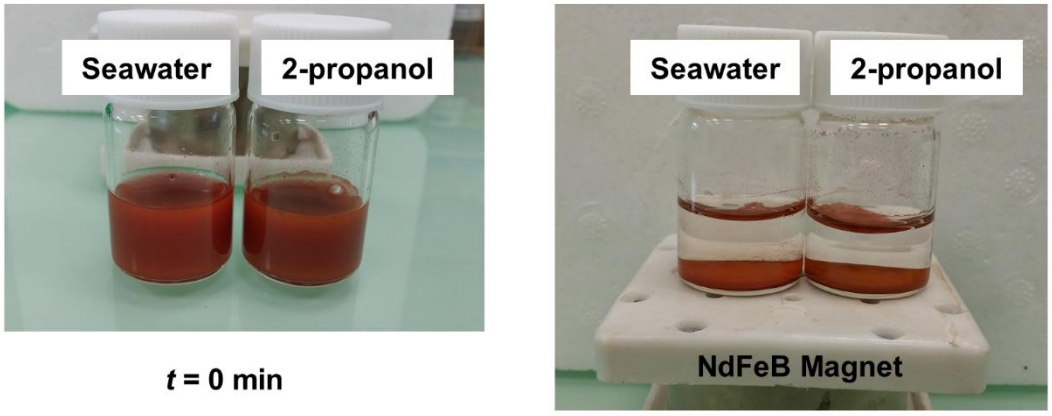

Figure S16.1. Image of 0.2-mTpBD-Me_2 dispersed in synthetic seawater and 2-propanol (left) and after magnetic separation (right) ([COF] = 1mg mL^{-1}).

17. References

(1) Z. Chen, B. Xing and W. B. McGill, *J. Environ. Qual.*, 1999, **28**, 1422–1428.

(2) E**.** Fux, C. Marcaillou, F. Mondeguer, R. Bire and P. Hess, *Harmful Algae*, 2008, **7**, 574–583.

(3) Z. Zendong, C. Herrenknecht, E. Abadie, C. Brissard, C. Tixier, F. Mondeguer, V. Séchet, Z. Amzil and P. Hess, *Toxicon*, 2014, **91**, 57–68.